Dielectric coatings for optimized low-loss saturable absorbers for high-power ultrafast laser

Liang Zhang (张 靓)[1,2*], Farina König[2], Joerg Neuhaus[2], Dominik Bauer[2], Thomas Dekorsy[2], and Yafu Chen (陈亚符)[1]

[1]*Department of Physics, Changchun University of Science and Technology, Changchun 130022, China*

[2]*Department of Physics and Center of Applied Photonics, University of Konstanz, 78457 Konstanz, Germany*

[*]*E-mail: zhangj@cust.edu.cn*

Received April 13, 2009

With the development of high power ultrafast laser passively mode-locked by a semiconductor saturable absorber mirror (SESAM), the damage threshold and degeneration mechanism of the SESAM become more and more important. One way to reduce the maximum electric field inside the active part of the SESAM is the use of a dielectric coating on the top of the semiconductor structure. With Fresnel formula, optical transfer matrix, and optical thin film theory, the electric field distribution and reflectance spectrum can be simulated. We introduce the design principles of SESAM including the dependence of reflectance spectrum on dielectric function of absorber, and investigate the dependences of the electric field distribution, modulation depth, reflectance spectrum, and the relative value of incident light power at the top quantum well of SESAM on the number of SiO_2/Ta_2O_5 layers.

OCIS codes: 140.7090, 140.4050, 320.7080.

doi: 10.3788/COL20090709.0819.

The integration of semiconductor saturable absorbers into a mirror structure results in a device that reflects more light when the more intense the light is. This device is called a semiconductor saturable absorber mirror (SESAM)[1]. Since 1992, SESAMs have become important for passive mode-locking of several solid-state lasers[2]. This invention offered new possibilities for passive solid-state mode-locking which extended the Q-switched pulses in nanosecond and picosecond regime to mode-locked pulses from tens of picoseconds to femtosecond. Moreover, Q-switch mode-locking (QML) instabilities were also overcome by the introduction of SESAMs. In contrast to Kerr lens mode-locking[3], the saturable absorber can be optimized independent of the cavity design, allowing successfull mode-locking to be achieved with a broad range of solid-state lasers and cavity designs. Moreover, compared with Kerr lens mode-locking, SESAMs have more flexibility in design to meet the required wavelength and saturation fluence.

From the earliest antiresonant Fabry-Perot semiconductor saturable absorber mirror[4] (A-FPSA) to high-finesse and low-finesse saturable absorber mirrors[5,6], saturable Bragg mirror[7], dispersion-compensating saturable absorber mirror[8], and low-loss broadband SESAM[9], the technology of SESAM has become more and more mature. By calculating the electric field distribution inside the semiconductor saturable mirror, the inserted location of the one or more quantum wells (QWs) within saturable absorber can be chosen to guarantee an effective saturable absorption, so that the reflectance spectrum is broadband, and a reflectivity enhancement can be obtained to meet the need of application. The simulation result can help us design SESAMs for good self-starting and stability of mode-locking.

In recent years, the pulse energy of ultrafast laser has been significantly improved. With the development of high power ultrafast lasers, such as femtosecond disk lasers with pulse energy beyond 10-μJ level[10,11], dielectric coating on the SESAM might resolve some issues that are caused by the large peak intensities inside the absorber structure[12]. One way to reduce the peak intensity in the SESAM is a coating on the top of a SESAM, which can protect the absorber layer from being damaged[13]. The structure of the dielectric must be designed, so that the coated films can protect the SESAM, while not influencing the characteristics of SESAM relevant for mode-locking at the same time.

The SESAM is designed according to the optical theory for designing multilayer films. The propagation of light through a multilayer film can be regarded as the interference of a forward going wave and a backward going wave[14]. The electric field distribution of light in the thin film layers can be calculated by Fresnel formula and optical transfer matrix method, so that the electric field distribution at any point inside or outside the whole device can be calculated, as well as the reflectance spectrum of the device.

It is the saturable absorber that helps the SESAM to realize the saturable absorption and support the self-starting and stabilization of mode-locking. To know the electric field distribution of light inside the whole structure is very important, since it defines the position to insert the saturable absorber. Theoretically, when the saturable absorber is located at the peak of the electric field of the incident light, the saturable absorption can be effectively realized. The number and position of the absorbing layers within the SESAM can thus be optimized according to the electric field distribution.

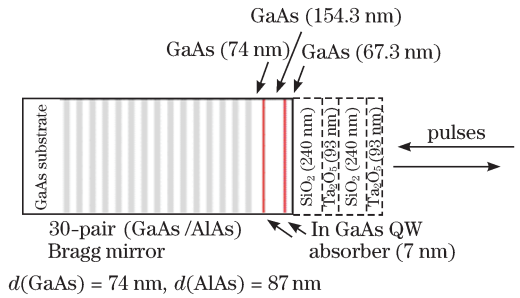

Fig. 1. Structure of SESAM.

The SESAM consists of three parts: the Bragg mirror, the active region including single or multiple QWs, and the top dielectric layer. The structure discussed below is designed close to the one used in Ref. [13].

The InGaAs QW plays a very important role in SESAM because of its saturable absorption characteristics. It absorbs light when the photon energy is sufficient to excite carriers from the valence band to the conduction band. Under strong excitation, the absorption is saturated because possible initial states of the pump transition are depleted, thus the reflectivity of SESAM is high. After the thermalization and recombination of the carriers, the absorption resumes. The modulation depth of the absorber should be controlled less than 3%, because larger modulation depth would result in Q-switch mode-locking. The Bragg mirror, the reflectivity of which should be above 98%−99%, helps SESAM have a high reflectivity for the defined wavelength. The thicknesses of GaAs space layers are designed in order to locate InGaAs QW at the peak of the standing wave, which results in the effective absorption of incident light. The important function of the SiO_2/Ta_2O_5 top reflector of the SESAM is to decrease the light energy that reaches the absorber layer, so that the absorber layer is not damaged by the large peak intensities of pulses inside a high power ultrafast laser. For example, in many cases, the light power is expected to be decreased by a half, that is, we need a top reflector consisting of a SiO_2/Ta_2O_5 Bragg mirror, which in these cases reflects about 50% of the incident light.

The structure of the SESAM is shown in Fig. 1. The whole structure was grown on a GaAs substrate. The Bragg mirror consists of 30 pairs GaAs/AlAs layers centered at the laser wavelength of 1030 nm for normal incidence. The active region consists of 7-nm-thick InGaAs QWs separated by GaAs barriers to place QWs into the antinodes of the standing wave pattern of the laser electric field. The dielectric coating consists of several pairs of alternating SiO_2 and Ta_2O_5 films with numerically optimized thicknesses for lower light intensity at QW position. The number of SiO_2/Ta_2O_5 pairs coated on the original SESAM is decided by the portion of incident light to be decreased. The reflectance spectrum should be around 1030 nm, which is the central emission wavelength of the Yb:YAG laser. The width of reflectance spectrum should be at least 100 nm.

The absorption of the InGaAs QW is based on the first interband transition between quantized hole and electron states. In order to model the absorption profile, a Lorentz model in combination with a step function can be assumed as a simple model for the combined densitiy of states including excitonic enhancement of the absorption.

For interband transitions where quantum mechanical expressions can be derived from the band structure of a material, one has only a formula for the imaginary part of the dielectric function. The missing real part can be constructed from the imaginary part using the Kramers-Kronig relation (KKR) that connects real and imaginary parts of susceptibilities. The Tauc-Lorentz model, which is an interband transition model, can give the expression for the imaginary part of the susceptibility[15]:

$$\chi_j(\omega) = \frac{1}{\omega}\frac{S^2\omega_0\omega_\tau(\omega-\omega_{\rm gap})^2}{(\omega^2-\omega_0^2)^2+\omega^2\omega_\tau^2}\Theta(\omega-\omega_{\rm gap}), \qquad (1)$$

where $\Theta(\omega-\omega_{\rm gap})$ is a step function for the two-dimensional (2D) density of states (DOS); S is related to the absorption strength, ω_τ is a damping coefficient which is mainly related to the modulation width, and they are both constant in the formula; ω_0 is the excitonic interband resonance frequency, and $\omega_{\rm gap}$ is the interband resonance without excitonic effects. By adjusting the parameters, the Lorentz model is used to fit the absorption spectrum of the SESAM to experimental static reflectivity data of the SESAM and hence give the modulation depth.

Figure 2 shows the dielectric function of the thin $In_{0.5}Ga_{0.5}As$ absorber, the refractive index of which is 3.3175, in the SESAM designed in this letter. It can be seen that the peak of the imaginary part is at the resonance wavelength of about 1030 nm. Below the gap at the right side, the imaginary part is exactly zero, that is, there is almost no absorption. Below the gap at the left side, the absorption, which is caused by the 2D DOS, is not zero.

In order to get sufficiently low insertion loss of a low-finesse A-FPSA, in which the top reflector is replaced by the Fresnel reflection semiconductor-air interface, the thickness of absorber has to be reduced by transparent space layers, such as GaAs for anti-resonance to be maintained. When the thickness of the absorber (QW) is less than $\lambda/2$, the standing wave effect has to be considered. The function of the transparent layers is to allow the thin absorber layer to shift to the appropriate position.

Figure 3 shows the electric field distribution of the standing wave inside and outside the SESAM. The simulation is performed by the SCOUT optical software[16]. The horizontal axis shows the position, and regards the

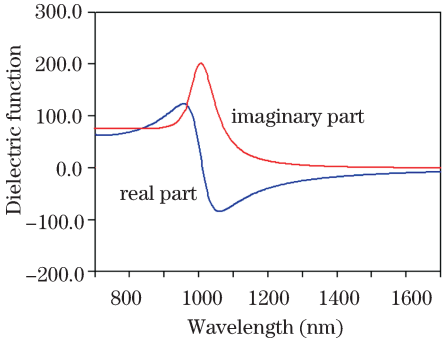

Fig. 2. Dielectric function of 7-nm $In_{0.5}Ga_{0.5}As$ absorber.

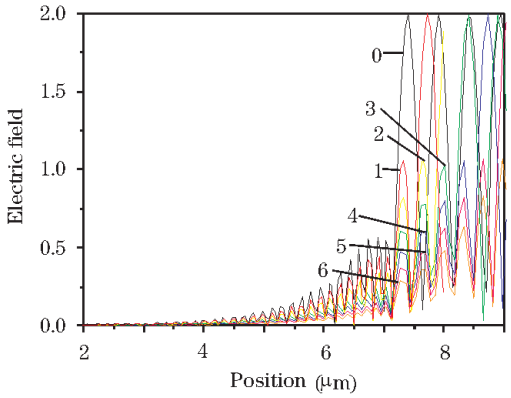

Fig. 3. Comparison of different electric field distributions inside SESAM with different dielectric structures. The curves stand for SESAMs with 0−6 pairs of SiO_2/Ta_2O_5 dielectric coatings.

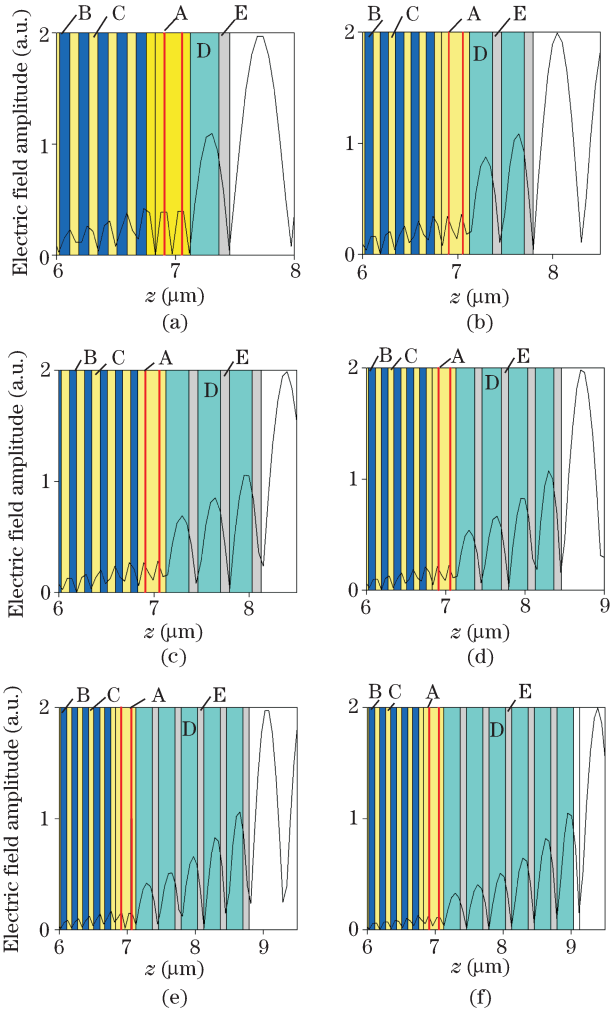

Fig. 4. Electric field distributions in SESAM. (a) − (f): correspond to SESAMs with 1− 6 pairs of SiO_2/Ta_2O_5 dielectric coating. Regions labeled with A: QW; B: AlAs; C: GaAs; D: SiO_2; E: Ta_2O_5.

bottom of substrate as the zero point. The curves depict the electric field intensities in different SESAMs with different numbers of SiO_2/Ta_2O_5 pairs coated on SESAM.

Every electric field distribution in Fig. 3 is shown in different pictures in Fig. 4. The electric field distributions of the standing wave inside the SESAM and the electric field intensity at the InGaAs QWs versus different antireflection layers with different numbers of SiO_2/Ta_2O_5 pairs can be clearly observed. In Fig. 4, every vertical line depicts an interface between layers, and the curves represent the electric field amplitude. It can be seen that the QWs are located almost exactly at the peak of electric field, and the dielectric layer can effectively decrease the incident light into the original SESAM.

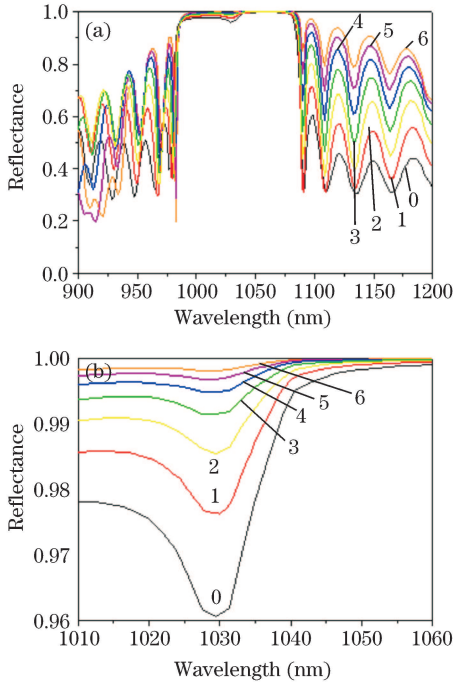

Fig. 5. (a) Comparison of reflectance spectra of SESAMs with 0−6 pairs of SiO_2/Ta_2O_5 dielectric coatings; (b) reflectance spectra around 1030 nm.

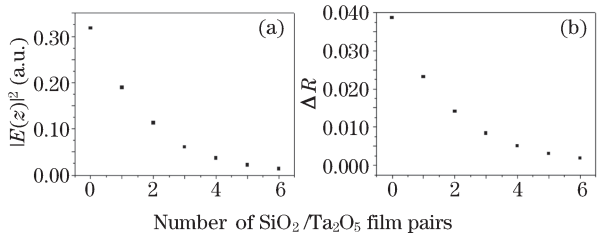

Fig. 6. (a) Squared magnitude of the electric field $|E(z)|^2$ at the top QW and (b) ΔR versus the number of SiO_2/Ta_2O_5 film pairs in the dielectric layer.

Figure 5 shows the reflectance spectra for SESAMs with two QWs and different dielectric structures. It can be seen that these structures can all have very high reflectivity ($> 90\%$) in the wavelength region of 985−1085 nm. The reflectivity bandwidths are wide ($\sim$ 100 nm), which supports the generation of picosecond or sub-picosecond ultra-short laser pulses. It can also be seen that the reflectance spectra have a small red shift with the increase of coated films. The asymmetry of reflectance spectra around 1030 nm is caused by the 2D DOS, which also causes the asymmetry of the imaginary part of the QW's dielectric function around 1030 nm shown in Fig. 2.

Figure 6(a) shows the squared magnitude of the electric field at the top QW versus the number of SiO_2/Ta_2O_5

pairs. It can be seen that when the dielectric coating consists of two pairs of alternating SiO_2/Ta_2O_5 layers deposited by electron beam evaporation, the field enhancement in the absorber can be reduced to less than 50% of its value in the uncoated device. Figure 6(b) shows the maximum change in nonlinear reflectivity ΔR[17] versus the number of SiO_2/Ta_2O_5 pairs. In SESAM mode-locked solid-state lasers, a very simple design guideline to prevent Q-switching instabilities is[17]

$$E_{\rm p}^2 > E_{\rm sat,L} E_{\rm sat,A} \Delta R, \tag{2}$$

where $E_{\rm p}$ is the intracavity pulse energy, $E_{\rm sat,L}$ is the saturation energy of the laser medium, and $E_{\rm sat,A}$ is the saturation energy of the saturable absorber. When the number of coating layers increases, $E_{\rm sat,A}$ also increases, while ΔR decreases at the same time, which means that Q-switching can be prevented.

The simulation of the electric field distribution inside the SESAM shows that with a dielectric coating of two pairs of SiO_2/Ta_2O_5 layers, the field enhancement in the absorber can be reduced to 50%. With this method, the number of film pairs to be coated as dielectric layers on the top of the SESAM can be chosen to meet the required reduction of light energy, which would be useful in the development of high power SESAM assisted mode-locking ultrafast laser.

This work was supported by the Ministry of Science, Research and Arts of Baden-Württemberg State of Germany and the Chinese Scholarship Council.

References

1. U. Keller, Nature **424,** 831 (2003).
2. U. Keller, K. J. Weingarten, F. X. Kärtner, D. Kopf, B. Braun, I. D. Jung, R. Fluck, C. Hönninger, N. Matuschek, and J. Aus der Au, IEEE J. Sel. Top. Quantum Electron. **2,** 435 (1996).
3. J. Wu, H. Cai, X. Han, and H. Zeng, Chin. Opt. Lett. **6,** 76 (2008).
4. L. R. Brovelli, U. Keller, and T. H. Chiu, J. Opt. Soc. Am. B **12,** 311 (1995).
5. U. Keller, D. A. B. Miller, G. D. Boyd, T. H. Chiu, J. F. Ferguson, and M. T. Asom, Opt. Lett. **17,** 505 (1992).
6. L. R. Brovelli, I. D. Jung, D. Kopf, M. Kamp, M. Moser, F. X. Kärtner, and U. Keller, Electron. Lett. **31,** 287 (1995).
7. S. Tsuda, W. H. Knox, E. A. de Souza, W. Y. Jan, and J. E. Cunningham, Opt. Lett. **20,** 1406 (1995).
8. D. Kopf, G. Zhang, R. Fluck, M. Moser, and U. Keller, Opt. Lett. **21,** 486 (1996).
9. Z. Zhang, T. Nakagawa, H. Takada, K. Torizuka, T. Sugaya, T. Miura, and K. Kobayashi, Opt. Commun. **176,** 171 (2000).
10. J. Neuhaus, J. Kleinbauer, A. Killi, S. Weiler, D. Sutter, and T. Dekorsy, Opt. Lett. **33,** 726 (2008).
11. J. Neuhaus, D. Bauer, J. Zhang, A. Killi, J. Kleinbauer, M. Kumkar, S. Weiler, M. Guina, D. H. Sutter, and T. Dekorsy, Opt. Express **16,** 20530 (2008).
12. C. Wang, Z. Han, Y. Jin, J. Shao, and Z. Fan, Chin. Opt. Lett. **6,** 773 (2008).
13. S. V. Marchese, C. R. E. Baer, A. G. Engqvist, S. Hashimoto, D. J. H. C. Maas, M. Golling, T. Südmeyer, and U. Keller, Opt. Express **16,** 6397 (2008).
14. J. Zhao, Z. Zhang, L. Chai, and Q. Wang, Chinese J. Lasers (in Chinese) **30,** 401 (2003).
15. G. E. Jellison, Jr., Thin Solid Films **313-314,** 33 (1998).
16. W. Theiss Hard- and Software, http://www.wtheiss.com/?c=1&content=products (Jan. 10, 2009).
17. C. Hönninger, R. Paschotta, F. Morier-Genoud, M. Moser, and U. Keller, J. Opt. Soc. Am. B **16,** 46 (1999).